GEOPHYSICS, VOL. 71, NO. 4 (JULY-AUGUST 2006); P. SI111–SI124, 17 FIGS.
10.1190/1.2211507

Spurious multiples in seismic interferometry of primaries

Roel Snieder[1], Kees Wapenaar[2], and Ken Larner[1]

ABSTRACT

Seismic interferometry is a technique for estimating the Green's function that accounts for wave propagation between receivers by correlating the waves recorded at these receivers. We present a derivation of this principle based on the method of stationary phase. Although this derivation is intended to be educational, applicable to simple media only, it provides insight into the physical principle of seismic interferometry. In a homogeneous medium with one horizontal reflector and without a free surface, the correlation of the waves recorded at two receivers correctly gives both the direct wave and the singly reflected waves. When more reflectors are present, a product of the singly reflected waves occurs in the crosscorrelation that leads to spurious multiples when the waves are excited at the surface only. We give a heuristic argument that these spurious multiples disappear when sources below the reflectors are included. We also extend the derivation to a smoothly varying heterogeneous background medium.

INTRODUCTION

Traditionally, imaging techniques are based on the illumination of an object by a coherent source. In many applications coherent sources are unavailable. Seismic interferometry is a technique in which the Green's function that describes the waves that propagate between two receivers is extracted by computing the correlation of signals recorded at these two receivers. These signals may have been excited by either coherent or incoherent sources. The advantages of this technique are that incoherent noise can be the source of the waves used for imaging and that one can, in effect, use a wavefield that is excited at one of the receivers, even though no physical source exists at that location.

The first formulation of this technique is from Claerbout (1968), who used the phrase *daylight imaging* because the daylight that we use in our vision also provides an incoherent illumination of the objects that we view. His derivation was applicable to horizontally layered media. The emergence of the Green's function was subsequently derived for 3D heterogeneous media of finite extent using normal-mode theory (Lobkis and Weaver, 2001). That derivation is applicable only for finite media that have a discrete frequency spectrum. This requirement was relaxed in an alternative derivation based on the representation theorem for one-way wave propagation (Wapenaar et al., 2002), and by using the general representation theorem (Weaver and Lobkis, 2004; Wapenaar, 2004). Alternative, but equivalent, proofs of the emergence of the Green's function have been formulated using the principle of time-reversal (Derode et al., 2003a, b; Roux and Fink, 2003). The relationship between these approaches is shown by Wapenaar et al. (2005).

The reconstruction of the Green's function from recordings of incoherent signals has been shown observationally using ultrasound (Weaver and Lobkis, 2001; Larose et al., 2004; Malcolm et al., 2004). Seismic interferometry has been used in helioseismology (Rickett and Claerbout, 1999; Rickett and Claerbout, 2000), in exploration seismology (Calvert et al., 2004; Bakulin and Calvert, 2004; Schuster, 2001; Schuster et al., 2004), in crustal seismology for the retrieval of the surface-wave Green's function (Campillo and Paul, 2003; Shapiro and Campillo, 2004; Shapiro et al., 2005), and for extracting the response of buildings from an incoherent excitation (Snieder and Şafak, 2006; Snieder et al., 2006).

The mechanism of seismic interferometry can be explained using the method of stationary phase (Snieder, 2004a; Roux et al., 2005). This is not surprising because the stationary-phase approximation is the natural tool to account for the destructive and constructive interference that forms the physical basis of seismic interferometry. The derivation of seismic interferometry based on stationary phase has also been used for waves in a waveguide (Sabra et al., 2005).

The derivation of stationary phase is applicable for simple media only where one can easily account for the different rays that propagate through the media. In this sense, the derivation based on stationary phase is less generally applicable than are derivations based on normal modes, representation theorems, or time-reversed imaging. Despite this limitation, the derivation based on stationary phase is

Manuscript received by the Editor April 1, 2005; revised manuscript received August 18, 2005; published online August 17, 2006.
[1]Center for Wave Phenomena, Colorado School of Mines, Department of Geophysics, Golden, Colorado 80401. E-mail: rsnieder@mines.edu; kenlarner@gmail.com.
[2]Delft Institute of Technology, Department of Geotechnology, Mijnbouwstraat 120, 2628 RX Delft, The Netherlands. E-mail: c.p.a.wapenaar@citg.tudelft.nl.

useful because it sheds light on the physics that underlies seismic interferometry. The value of such a derivation is mostly didactic, but it also highlights sampling issues and the generation of spurious multiples.

Here we show that singly reflected waves that propagate between two receivers in the subsurface can correctly be reproduced by correlating the waves that have been excited by uncorrelated sources at the surface and are recorded at the two receivers. We first derive this for the simplest case of a homogeneous medium without a free surface and horizontal reflectors in the subsurface, and, in Appendix A, treat a medium that is heterogeneous above the reflectors.

In the next section, we derive the general framework for illumination of the subsurface by incoherent sources, and introduce the employed single-scattering model in the subsequent section. In the section Analysis of term $T1$, we show how this leads to the retrieval of the direct wave that propagates between the receivers, and, in the section Analysis of terms $T2$ and $T3$, we show that this procedure also correctly leads to the singly reflected wave that propagates between the receivers. The correlation of the singly reflected waves leads to a contribution that is proportional to the square of the reflection coefficient. We show in the section Analysis of term $T4$ that this term is kinematically equivalent to the direct wave that propagates between the receivers. We next show a numerical example that illustrates the role of stationary phase in seismic interferometry, and generalize the derivation to the case of a layered medium with more than one reflector to show that the product of singly reflected waves from different reflectors gives a nonzero contribution to the crosscorrelation. We refer to these terms as *spurious multiples* because these terms depend on the product of reflection coefficients, just as do real multiples. The spurious multiples, however, have arrival times that differ from those of real multiples.

ILLUMINATING THE SUBSURFACE FROM SOURCES ALONG A SURFACE

Consider the problem wherein sources along the surface $z = 0$ illuminate the subsurface. We consider a pressure field p that is related to a volume injection source S by

$$\nabla \cdot \left(\frac{1}{\rho} \nabla p \right) + \frac{\omega^2}{K} p = S, \tag{1}$$

where ρ denotes the mass density, K the bulk modulus, and ω the angular frequency. The sources S can be either temporally coherent or incoherent, and they may act either simultaneously or sequentially. The sources are placed at locations $\mathbf{r}_S = (x,y,0)$ and have a source time signal $S_S(t)$ that corresponds in the frequency domain to the complex spectrum $S_S(\omega)$. The earth response that is excited by these sources is recorded at two receivers at locations $\mathbf{r}_A = (x_A,0,z_A)$ and $\mathbf{r}_B = (x_B,0,z_B)$, respectively. Without loss of generality, we have aligned the x-axis of the employed coordinate system with the projection of receiver positions onto the horizontal; hence, in this coordinate system the y-coordinate of both receivers vanishes.

The source time-functions $S_S(t)$ may be impulsive, but they might also correspond to functions with a more random character, as would be excited by, for example, traffic noise in a land survey or turbulent wave noise at the sea-surface. In the sequel, we assume that the source time-functions for sources at $\mathbf{r}_S$ and $\mathbf{r}_{S'}$ are uncorrelated when averaged over time and that the power spectra of the source time functions are identical:

$$\int_0^{T_{\text{aver}}} S_S(t) S_{S'}(t+\tau) dt = \delta_{SS'} C(\tau), \tag{2}$$

where T_{aver} denotes the length of time averaging and $C(\tau)$ the autocorrelation of the source time functions. The autocorrelation is the Fourier transform of the power spectrum. Because all sources are assumed to have the same power spectrum, they have the same autocorrelation as well.

The source time-functions may have a different character in different imaging experiments. In the controlled virtual-source experiments of Calvert et al. (2004) and Bakulin and Calvert (2004), the shots do not overlap in time. The shots are recorded and processed one after the other, and the cross terms between the shots in expression 2, by definition, vanish. For continuous sources with a random character, the integral in equation 2 vanishes for different sources ($S \neq S'$) when the source time-functions are uncorrelated and the averaging time T_{aver} is sufficiently large (Snieder, 2004a). Expression 2 corresponds in the frequency domain to

$$S_S(\omega) S^*_{S'}(\omega) = \delta_{SS'} |S(\omega)|^2. \tag{3}$$

We now consider correlation of the waves recorded at two receivers for the special case of an acoustic medium. The waves recorded at the receivers A and B are given by

$$u_A(\omega) = \sum\nolimits_S G^{\text{full}}(\mathbf{r}_A, \mathbf{r}_S, \omega) S_S(\omega),$$
$$u_B(\omega) = \sum\nolimits_{S'} G^{\text{full}}(\mathbf{r}_B, \mathbf{r}_{S'}, \omega) S_{S'}(\omega), \tag{4}$$

with G^{full} the full Green's function, which consists of the direct wave, primaries, and multiples. In the frequency domain, the temporal correlation of these waves is given by

$$C_{AB}(\omega) = u_A(\omega) u^*_B(\omega), \tag{5}$$

where the asterisk denotes the complex conjugate. Inserting equation 4 into equation 5 gives

$$C_{AB}(\omega) = \sum_{S,S'} G^{\text{full}}(\mathbf{r}_A, \mathbf{r}_S) G^{\text{full}*}(\mathbf{r}_B, \mathbf{r}_{S'}) S_S(\omega) S^*_{S'}(\omega). \tag{6}$$

Since the sources are uncorrelated, as stated in expression 3, the cross-terms $S \neq S'$ in this double sum vanish; hence,

$$C_{AB}(\omega) = \sum_{S} G^{\text{full}}(\mathbf{r}_A, \mathbf{r}_S) G^{\text{full}*}(\mathbf{r}_B, \mathbf{r}_S) |S(\omega)|^2. \tag{7}$$

When the sources are densely and uniformly distributed along the surface, with n sources per unit surface area, the sum over sources can be replaced by an integration: $\Sigma_S(\ldots) \rightarrow n \int (\ldots) dxdy$ over the surface. This gives

$$C_{AB}(\omega) = |S(\omega)|^2 n \int G^{\text{full}}(\mathbf{r}_A, \mathbf{r}_S) G^{\text{full}*}(\mathbf{r}_B, \mathbf{r}_S) dxdy, \tag{8}$$

with x and y the coordinates of the surface source (Figure 1).

A SINGLE-SCATTERING MODEL

To help understand the physics of seismic interferometry, we first illustrate this technique with a model that consists of a single horizontal reflector, with a reflection coefficient for downward-arriving waves r, that is embedded in a homogeneous medium. The far-field reflection coefficient r is equal to the plane-wave reflection coefficient. This coefficient depends, in general, on the angle of incidence θ. The Green's function in the homogeneous medium is given by

$$G(R) = -\rho\frac{e^{ikR}}{4\pi R}, \tag{9}$$

with the wavenumber $k = \omega/v$, v the wave velocity, and R the distance of propagation (Snieder and Chapman, 1998). We presume that there is no free surface, so this model does not include any multiply reflected waves. As shown in Figure 1, $\mathbf{r}_{RA}$ denotes the reflection point of the wave that propagates to $\mathbf{r}_A$. The full Green's function is the superposition of the direct wave and the singly reflected wave:

$$\begin{aligned} G^{full}(\mathbf{r}_A,\mathbf{r}_S) &= G(|\mathbf{r}_A - \mathbf{r}_S|) + rG(|\mathbf{r}_A - \mathbf{r}_{RA}| + |\mathbf{r}_{RA} - \mathbf{r}_S|), \\ G^{full}(\mathbf{r}_B,\mathbf{r}_S) &= G(|\mathbf{r}_B - \mathbf{r}_S|) + rG(|\mathbf{r}_B - \mathbf{r}_{RB}| + |\mathbf{r}_{RB} - \mathbf{r}_S|). \end{aligned} \tag{10}$$

In this expression, we assumed that the reflected wave is given by the product of the reflection coefficient and the Green's function that accounts for the propagation from the source to an image point of the receiver below the reflector. The image points of the receivers A and B are indicated in Figure 1 by $\mathbf{r}'_A$ and $\mathbf{r}'_B$, respectively. As shown in that figure, for receiver A the total distance covered by the reflected wave is $|\mathbf{r}_A - \mathbf{r}_{RA}| + |\mathbf{r}_{RA} - \mathbf{r}_S|$.

Inserting equation 10 into expression 8 gives an expression for the correlation, which consists of a sum of four terms:

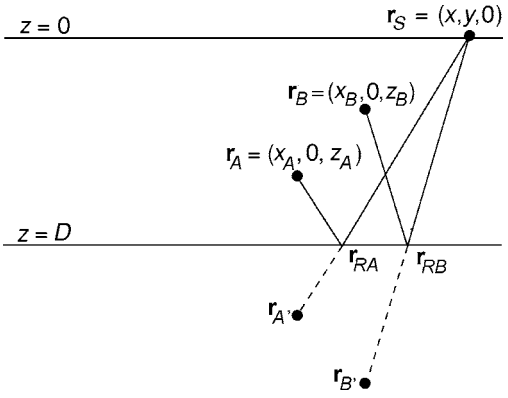

Figure 1. The geometry of an imaging experiment with a source at the surface and two receivers at $\mathbf{r}_A$ and $\mathbf{r}_B$. The mirror images of these receivers in the reflector are indicated at the locations $\mathbf{r}_{A'}$ and $\mathbf{r}_{B'}$, respectively.

$$\begin{aligned} C_{AB}(\omega) = n|S(\omega)|^2 &\underbrace{\int G(|\mathbf{r}_A - \mathbf{r}|)G^*(|\mathbf{r}_B - \mathbf{r}|)dxdy}_{T1} \\ &+ n|S(\omega)|^2\mathbf{r}\underbrace{\int G(|\mathbf{r}_A - \mathbf{r}_{RA}| + |\mathbf{r}_{RA} - \mathbf{r}|)G^*(|\mathbf{r}_B - \mathbf{r}|)dxdy}_{T2} \\ &+ n|S(\omega)|^2\mathbf{r}\underbrace{\int G(|\mathbf{r}_A - \mathbf{r}|)G^*(|\mathbf{r}_B - \mathbf{r}_{RB}| + |\mathbf{r}_{RB} - \mathbf{r}|)dxdy}_{T3} \\ &+ n|S(\omega)|^2\mathbf{r}^2\underbrace{\int G(|\mathbf{r}_A - \mathbf{r}_{RA}| + |\mathbf{r}_{RA} - \mathbf{r}|)G^*(|\mathbf{r}_B - \mathbf{r}_{RB}| + |\mathbf{r}_{RB} - \mathbf{r}|)dxdy}_{T4}. \end{aligned} \tag{11}$$

Term $T1$ is the correlation of the direct waves that propagate to the two receivers. This term does not depend on the reflection coefficient. Terms $T2$ and $T3$ are proportional to the reflection coefficient r. For this reason they can be expected to account for the singly reflected waves in the Green's function that are extracted from the correlation. Term $T4$ depends on r^2. In the following, we analyze terms $T1$–$T4$ in order to establish the connection between the correlation and the Green's function for this simple wave-propagation problem.

ANALYSIS OF TERM $T1$

The derivation shown in this section is similar to that in an earlier analysis (Snieder, 2004a). Using the lengths L_A and L_B, as defined in Figure 2, and the Green's function 9, we can write term $T1$ as

$$T1 = \frac{\rho^2}{(4\pi)^2}\int\frac{\exp(ik(L_A - L_B))}{L_A L_B}dxdy. \tag{12}$$

The integrand has an oscillatory character with, as we will see, a stationary point. For this reason we analyze this integral in the stationary-phase approximation. This approximation is based on the assumption that the amplitude of the integrand varies smoothly compared to the phase. The dominant contribution(s) to the integral comes from the point(s) where the phase is stationary (Bleistein, 1984; Snieder, 2004b). The stationary phase approximation is based on a second order Taylor expansion of the exponent (e.g., equation 24.51 of Snieder, 2004b), and an analytic evaluation of the resulting integrand (e.g., expression 24.38 of Snieder, 2004b).

In Figure 2, the lengths $L_{A,B}$ are given by

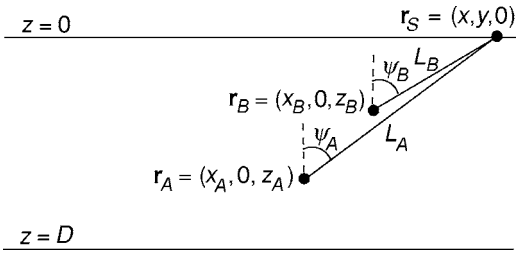

Figure 2. Definition of the geometric variables in the analysis of term $T1$.

$$L_{A,B} = \sqrt{(x - x_{A,B})^2 + y^2 + z_{A,B}^2}. \quad (13)$$

The stationary point of the integrand follows by setting the partial x- and y-derivatives of $L = L_A - L_B$ equal to zero. For the y-derivative this gives

$$0 = \frac{\partial L}{\partial y} = \frac{y}{L_A} - \frac{y}{L_B}. \quad (14)$$

This derivative vanishes for $y = 0$; hence the condition of stationarity with respect to y implies that the stationary source point lies in the vertical plane of the receivers. The stationarity condition with respect to the x-coordinate gives

$$0 = \frac{\partial L}{\partial x} = \frac{x - x_A}{L_A} - \frac{x - x_B}{L_B} = \sin\psi_A - \sin\psi_B, \quad (15)$$

where the angles ψ_A and ψ_B are defined in Figure 2. The phase thus is stationary only when

$$\psi_A = \psi_B \quad \text{and} \quad y = 0. \quad (16)$$

The stationarity condition $\psi_A = \psi_B$ is illustrated in Figure 3. It implies that the one and only stationary source point at the surface is aligned with the line joining the two receivers. In these figures, the receivers are at different depths. Note that when the receivers are at the same depth ($z_A = z_B$) there is no stationary source position, except for sources infinitely far away. Any attenuation will suppress the contribution of those sources.

Kinematically, expression 12 gives a contribution at a lag time that is equal to the time it takes for the wave to propagate from receiver B to receiver A. This is because the wave that propagates along the path shown in Figure 3 arrives at receiver A with a time delay $|\mathbf{r}_A - \mathbf{r}_B|/v$ compared to the wave that arrives at receiver B. It is nontrivial that the evaluation of the integral in expression 12 gives a contribution that is also dynamically equal to the Green's function of the waves that propagate between the receivers A and B. In the following, we evaluate the integral in the stationary-phase approximation.

Evaluating the second derivatives of $L = L_A - L_B$ while using expression 16 for the stationary point gives

$$\frac{\partial^2 L}{\partial x^2} = \frac{z_A^2}{L_A^3} - \frac{z_B^2}{L_B^3} = \frac{z_A^2}{L_A^2}\frac{1}{L_A} - \frac{z_B^2}{L_B^2}\frac{1}{L_B} = \cos^2\psi\left(\frac{1}{L_A} - \frac{1}{L_B}\right) \quad (17)$$

and

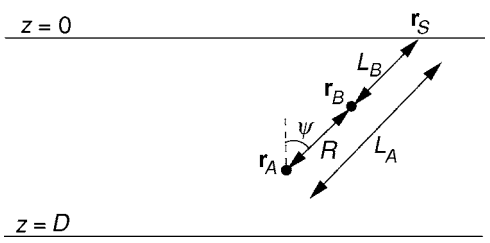

Figure 3. Definition of the geometric variables for the stationary source position in term $T1$.

$$\frac{\partial^2 L}{\partial y^2} = \frac{L_A^2}{L_A^3} - \frac{L_B^2}{L_B^3} = \frac{1}{L_A} - \frac{1}{L_B}. \quad (18)$$

In this example and the following examples, $\partial^2 L/\partial x\partial y = 0$ at the stationary point, and the 2D stationary-phase integral reduces to the product of two 1D stationary-phase integrals over the x- and y-coordinates, respectively.

In the following, L_A and L_B are the path lengths for the stationary source position as shown in Figure 3. Note that in the geometry of Figure 3, $L_A > L_B$ so that $L_A^{-1} - L_B^{-1} < 0$. Evaluating integral 12 in the stationary-phase approximation thus gives

$$T1 = \frac{\rho^2}{(4\pi)^2}\frac{\exp(ik(L_A - L_B))}{L_A L_B} \times e^{-i\pi/4}\sqrt{\frac{2\pi}{k}}\frac{1}{\sqrt{\cos^2\psi\left(\frac{1}{L_B} - \frac{1}{L_A}\right)}}e^{-i\pi/4} \times \sqrt{\frac{2\pi}{k}}\frac{1}{\sqrt{\frac{1}{L_B} - \frac{1}{L_A}}}. \quad (19)$$

In this derivation, we assume that $\omega > 0$; hence $k > 0$. For negative frequencies the integral can be found by complex conjugation. Using the relation $k = \omega/v$, we can write expression 19 as

$$T1 = \frac{-i\rho^2 v}{8\pi\omega\cos\psi}\frac{\exp(ik(L_A - L_B))}{L_A - L_B}. \quad (20)$$

The distance $L_A - L_B$ is equal to the receiver separation R shown in Figure 3. With expression 9 and including the factor $n|S(\omega)|^2$ of expression 11, this gives a total contribution that is equal to

$$T1 = \frac{n|S(\omega)|^2\rho v}{2\cos\psi} \times \frac{G(R)}{-i\omega}. \quad (21)$$

This means that the contribution of term $T1$ to the correlation is, in the frequency domain, proportional to the Green's function of the direct wave that propagates between the receivers. Note that this Green's function is multiplied by the source density n at the surface. A denser source distribution gives a stronger correlation than does a less dense one. The Green's function is also multiplied by the power spectrum $|S(\omega)|^2$ of the sources, and one needs to correct for this term. The impedance term ρv is also present in the general derivation of Wapenaar et al. (2005). In order to retrieve the Green's function from term $T1$, one also needs to multiply with $-i\omega$. Because of the employed Fourier transform, $f(t) = \int F(\omega)\exp(-i\omega t)d\omega$, this multiplication corresponds to a differentiation in the time domain. This differentiation corrects for the integration that is carried out in the crosscorrelation. This need to carry out the differentiation was also noted in other formulations of seismic interferometry (e.g., Lobkis and Weaver, 2001; Snieder, 2004a; Weaver and Lobkis, 2004). The term $\cos\psi$ in the denominator is an obliquity factor that corrects for the fact that the length element QQ' of Figure 4 perpendicular to the ray corresponds to a line element PP' along the surface whose length is given by $PP' = QQ'\cos\psi$.

Consider the case that the sources on the surface $z = 0$ are placed along just the line $y = 0$ rather than over the surface. Then there is no integration over the y-coordinate, and the terms in expression 19 that

come from the y-integration are absent; in that case,

$$T1_{\text{line}} = \frac{in|S(\omega)|^2\rho\sqrt{v}}{\sqrt{8\pi}\sqrt{-i\omega}\cos\psi}\sqrt{\frac{1}{L_B}-\frac{1}{L_A}}G(R). \quad (22)$$

Note the presence of the factor i and the term $1/\sqrt{-i\omega}$. Correcting for these terms therefore involves a Hilbert transform and a fractional derivative. These correction factors are common in two-dimensional imaging experiments (Yilmaz, 1987; Bleistein et al., 2001; Haney et al., 2005). Without these corrections the reconstructed Green's function does not have the proper phase and frequency dependence. More seriously, in contrast to equation 21, expression 22 depends explicitly on the distances L_A and L_B. It turns out that when the derivation leading to expression 22 is repeated using the Green's function in 2D, an expression analogous to equation 21 is obtained. The presence of the fractional derivatives and the lengths L_A and L_B is thus due to a mismatch between the dimensionality of the physical space through which the waves propagate (3D versus 2D) and the dimensionality of the source distribution (2D versus 1D). The derivation of seismic interferometry by Roux and Fink (2003) is based on wave propagation in 3D, while the employed sources are placed along a line. As shown by the example of expression 22, this leads to a Green's function that is kinematically correct, but whose amplitude and phase are not.

The analysis of this section can be generalized for a heterogeneous medium in which the velocity is sufficiently smooth to warrant the use of ray theory. We show in Appendix A that term $T1$ is then given by

$$T1 = \sum_{\text{stat. points}} \frac{n|S(\omega)|^2\rho_S v_S}{2\cos\psi} \times \frac{G^{ray}(\mathbf{r}_A,\mathbf{r}_B)}{-i\omega}, \quad (23)$$

where $G^{\text{ray}}(\mathbf{r}_A,\mathbf{r}_B)$ is the ray-geometric Green's function for the waves recorded at $\mathbf{r}_A$ that are generated by a point source at $\mathbf{r}_B$. The summation in this expression is over all the stationary source points on the surface $z = 0$. These points can be found by tracing rays from $\mathbf{r}_A$ to $\mathbf{r}_B$ and by extending these rays to the surface $z = 0$. Because in general more than one ray may connect the receivers, there may be more than one stationary point. The angle ψ is the angle between these rays at the surface and the vertical, while v_S and ρ_S are the velocity and density, respectively, at the intersection of these rays with the surface.

ANALYSIS OF TERMS $T2$ AND $T3$

The analysis of terms $T2$ and $T3$ is achieved by applying the theory of the previous sections to receivers at the image points $\mathbf{r}_{A'}$ and $\mathbf{r}_{B'}$ of Figure 1. Here we show explicitly that the crosscorrelation correctly produces the singly reflected waves. With the lengths defined in Figure 4–6, term $T2$ is given by

$$T2 = \frac{\rho^2}{(4\pi)^2}\int \frac{\exp(ik(L_1+L_2-L_B))}{(L_1+L_2)L_B}dxdy. \quad (24)$$

This integral can be also evaluated in the stationary-phase approximation. The lengths L_1, L_2, and L_B, and their derivatives with respect to the source position are derived in Appendix B. As shown there, the phase is stationary when the source position satisfies

$$\theta_A = \psi_B \quad \text{and} \quad y = 0. \quad (25)$$

This condition is depicted in Figure 6: The net result of waves radiated from the stationary source position at the surface $z = 0$ correspond to the straight raypath from the source through receiver B via a specular reflection to receiver A. Just as in the analysis of term $T1$, the time delay of this wave recorded at the two receivers is now equal to the time it takes the wave to travel from receiver B via the reflector to receiver A. Thus the correlation is kinematically equal to the Green's function for the reflected waves. With the following stationary-phase evaluation of integral 24, we verify that the retrieved Green's function is also dynamically correct.

As shown in Appendix B, the second derivatives of $L = L_1 + L_2 - L_B$ with respect to the source position are given by

$$\frac{\partial^2 L}{\partial x^2} = \cos^2\theta\left(\frac{1}{L_1+L_2}-\frac{1}{L_B}\right) \quad (26)$$

and

$$\frac{\partial^2 L}{\partial y^2} = \frac{1}{L_1+L_2}-\frac{1}{L_B}. \quad (27)$$

In expressions 26 and 27, it is understood that all lengths are evaluated at the stationary point.

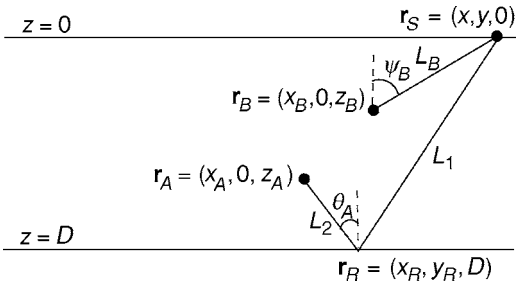

Figure 5. Definition of the geometric variables in the analysis of term $T2$.

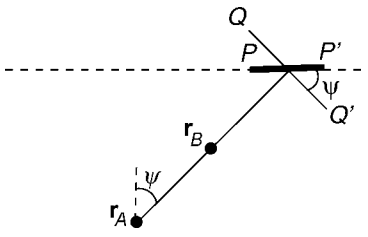

Figure 4. The relationship between an element PP' along the surface and the corresponding element QQ' perpendicular to the receiver line.

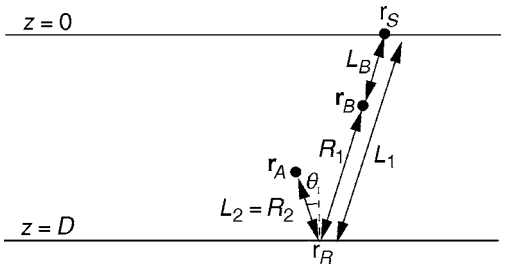

Figure 6. Definition of the geometric variables for the stationary source position in the analysis of term $T2$.

The stationary-phase evaluation of integral 24 can now be carried out. Keeping in mind that $(L_1 + L_2)^{-1} - L_B^{-1} < 0$, and using the same steps as in the section Analysis of term $T1$, gives

$$T2 = \frac{\rho^2}{(4\pi)^2}\frac{\exp(ik(L_1 + L_2 - L_B))}{(L_1 + L_2)L_B}(e^{-i\pi/4})^2\frac{2\pi}{k\cos\theta} \times\left(\frac{1}{L_B} - \frac{1}{L_1 + L_2}\right)^{-1}. \quad (28)$$

As shown in Figure 6, $L_1 - L_B = R_1$, and $L_2 = R_2$. With definition 9 for the Green's function, this gives, after taking the $rn|S(\omega)|^2$ terms into account,

$$T2 = \frac{n|S(\omega)|^2\rho v}{2\cos\theta} \times r\frac{G(R_1 + R_2)}{-i\omega}. \quad (29)$$

Note the resemblance with expression 21 for the contribution of term $T1$ which gives the direct wave that propagates between the receivers. Expression 29 shows that the contribution of term $T2$ leads to the singly-reflected wave that propagates from receiver B via the reflector to receiver A. The same corrections must be applied to term $T2$ as to term $T1$, as discussed in the section Analysis of term $T1$.

The same analysis can be applied to term $T3$ of expression 11, resulting in the complex conjugate of expression 29, so that

$$T3 = \frac{n|S(\omega)|^2\rho v}{2\cos\theta} \times r\left(\frac{G(R_1 + R_2)}{-i\omega}\right)^*. \quad (30)$$

The stationary point now lies at the location on the surface such that the direct wave from the source to receiver A propagates along the same path as the wave that travels from the source to the reflector, and ultimately to receiver B.

The Green's function in expression 29 is the causal Green's function, while its complex conjugate in equation 30 is the acausal one. It is known that seismic interferometry gives the superposition of the causal and the acausal Green's functions (Lobkis and Weaver, 2001; Derode et al., 2003a, b; Malcolm et al., 2004). The causal Green's function can be retrieved from the cross-correlation either by truncating the cross-correlation for $t < 0$, or by averaging the cross-correlation for negative times and positive times.

ANALYSIS OF TERM $T4$

For the analysis of term $T4$, we carry out the stationary-phase analysis of the integral

$$T4 = \frac{\rho^2}{(4\pi)^2}\int\frac{\exp(ik(|\mathbf{r}_A - \mathbf{r}_{RA}| + |\mathbf{r}_{RA} - \mathbf{r}_S| - |\mathbf{r}_B - \mathbf{r}_{RB}| - |\mathbf{r}_{RB} - \mathbf{r}_S|))}{(|\mathbf{r}_A - \mathbf{r}_{RA}| + |\mathbf{r}_{RA} - \mathbf{r}_S|)(|\mathbf{r}_B - \mathbf{r}_{RB}| + |\mathbf{r}_{RB} - \mathbf{r}_S|)}dxdy, \quad (31)$$

where all variables are defined in Figure 7. The stationary point follows from setting the x- and y-derivatives of the phase equal to zero. As in the previous sections, the stationarity condition with respect to y leads to the condition $y = 0$. This means again that the stationary point lies in the vertical plane of the receivers. Using the same steps that lead to expression B-10 of Appendix B, one finds that the stationarity condition with respect to x is given by

$$0 = \frac{\partial L}{\partial x} = \sin\theta_A - \sin\theta_B, \quad (32)$$

where the angles θ_A and θ_B are defined in Figure 7. The point of stationary phase thus is defined by the conditions

$$\theta_A = \theta_B \quad \text{and} \quad y = 0. \quad (33)$$

This condition of stationary phase corresponds to the source position shown in Figure 8. The stationary source position launches a wave that, after specular reflection at the interface, propagates along the line that joins the receivers. Because the reflected waves are each proportional to r, this contribution to the correlation is proportional to r^2. The correlation of the waves shown in Figure 8 is nonzero for a lag-time that is equal to the time it takes for the waves to propagate between the receivers. Kinematically, term $T4$ can thus be expected to correspond to the Green's function of the direct wave that propagates between the receivers.

In order to carry out the stationary-phase analysis, the second derivatives of the phase are needed. These derivatives follow from expressions B-11, B-12, B-16, and B-17 with the lengths defined in Figure 8. Term $T4$ is then given in the stationary-phase approximation by

$$T4 = \frac{\rho^2}{(4\pi)^2}\frac{\exp(ik(L_1 + L_{2A} - L_1 - L_{2B}))}{(L_1 + L_{2A})(L_1 + L_{2B})}(e^{-i\pi/4})^2 \times\frac{2\pi}{k\cos\psi}\left(\frac{1}{L_1 + L_{2A}} - \frac{1}{L_1 + L_{2B}}\right)^{-1}, \quad (34)$$

where we used the same angle θ for the stationary source position as the angle ψ of Figure 3. According to the geometry of Figure 8, $R = L_{2B} - L_{2A}$. With definition 9 for the Green's function, this gives, after taking the $r^2n|S(\omega)|^2$ terms into account,

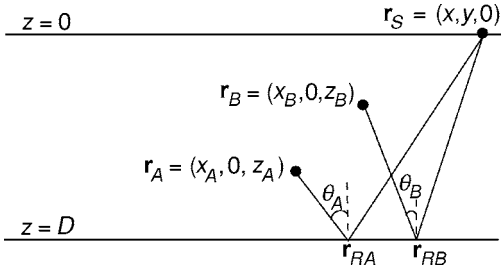

Figure 7. Definition of the geometric variables in the analysis of term $T4$.

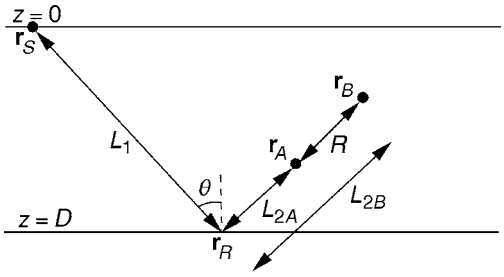

Figure 8. Definition of the geometric variables in the analysis of term $T4$ for the stationary source position.

$$T4 = \frac{n|S(\omega)|^2\rho v}{2\cos\psi} \times r^2\left(\frac{G(R)}{-i\omega}\right)^*. \qquad (35)$$

Apart from the r^2-term and a complex conjugation of the Green's function, term $T4$ is similar to term $T1$ as given in expression 21. The r^2-term arises because both of the waves that are reflected upward from the reflector are proportional to the reflection coefficient. The complex conjugate appears because the wave arrives at receiver A before it hits receiver B.

Theory predicts that seismic interferometry leads to the superposition of the causal and acausal Green's functions (Wapenaar, 2004; van Manen et al., 2005). In the frequency domain, this corresponds to the superposition of the Green's function and its complex conjugate. Note that because of the r^2-factor, the term $T4$ is not equal to the complex conjugate of term $T1$ in equation 21. This discrepancy can be explained as follows. Theory predicts that the sum of the causal and acausal Green's function is obtained when sources are present on a closed surface that surrounds the medium (Wapenaar, 2004; van Manen et al., 2005). This closed surface includes sources that are placed below the reflector. Let us consider the simplest case where the reflection is caused by a density contrast only. Sources below the reflector give a stationary-phase contribution to term $T4$ that is given by

$$T_{\text{below}} = \frac{n|S(\omega)|^2\rho_b v}{2\cos\psi} \times t^2\left(\frac{G(R)}{-i\omega}\right)^*, \qquad (36)$$

with t the transmission coefficient for waves incident from below the reflector, and where ρ_b is the density below the reflector. In that case, the reflection coefficient is given by $r = (\rho_b - \rho)/(\rho_b + \rho)$, and the transmission coefficient for upward traveling waves is equal to $t = 2\rho/(\rho_b + \rho)$, hence $\rho r^2 + \rho_b t^2 = \rho$. Using this result, expressions 35 and 36 combine to give a total contribution

$$T4 + T_{\text{below}} = \frac{n|S(\omega)|^2\rho v}{2\cos\psi} \times \left(\frac{G(R)}{-i\omega}\right)^*. \qquad (37)$$

This gives the upward traveling Green's function between the receivers.

INTERPRETATION OF TERMS $T1$-$T4$

Inserting expressions 21, 29, 30, and 35 into equation 11 gives for a single horizontal reflector, the following total contribution to the correlation:

$$C_{AB}(\omega) = \frac{1}{2}n|S(\omega)|^2\rho v\left\{\frac{G(R)}{-i\omega\cos\psi} + r\frac{G(R_1+R_2)}{-i\omega\cos\theta} + r\left(\frac{G(R_1+R_2)}{-i\omega\cos\theta}\right)^* + r^2\left(\frac{G(R)}{-i\omega\cos\psi}\right)^*\right\}. \qquad (38)$$

The correlation is thus proportional to a weighted average of the causal and acausal Green's function for the direct wave and the singly reflected waves. In practical applications of seismic interferometry in reflection seismology, this contribution to the direct waves is not relevant because primary reflections rather than direct waves are used to image the subsurface.

The four terms in expression 38 correspond to the waves that propagate along the four trajectories shown in Figure 9. The waves in diagrams (a) and (b) are the direct waves that propagate in opposite directions between the two receivers. The waves in diagrams (c) and (d) are the singly reflected waves that propagate in opposite directions between the receivers. These diagrams provide an illustration of why the correlation leads to the superposition of the causal and acausal Green's function.

A NUMERICAL EXAMPLE

For simplicity, consider the theory in two dimensions. A reflector with the reflection coefficient $r = 0.8$ is located at a depth 1500 m below the surface. This is not a small reflection coefficient, but since there is only one reflector and no free surface, this model generates no multiple reflections, regardless of how large the reflection coefficient is. The wave velocity is $v = 2000$ m/s, and the receivers are located at $\mathbf{r}_A = (0, 1000)$ m and $\mathbf{r}_B = (300, 500)$ m, respectively. We used sources at the surface with a spacing $\Delta x = 20$ m, and a Ricker wavelet with a dominant frequency of 50 Hz for $S(\omega)$.

The contributions of the sources at the surface $z = 0$ to terms $T1$-$T4$ is shown in Figure 10a, while the sum over all source positions is shown in Figure 10b. Figure 10b shows four distinct arrivals. Arriv-

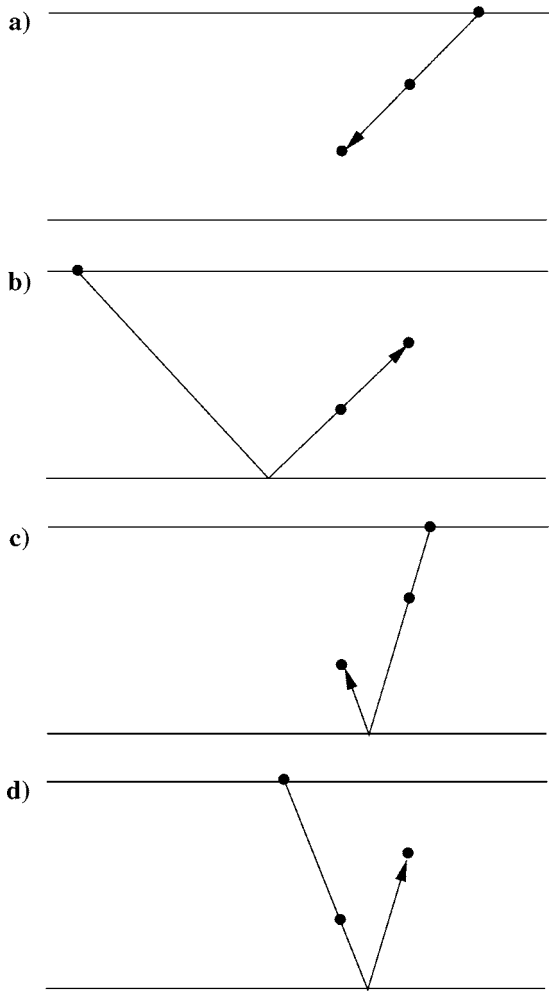

Figure 9. The raypaths corresponding to the stationary contributions to the correlations for the causal direct wave from term $T1$ (a), the acausal direct wave from term $T4$ (b), the causal reflected wave from term $T2$ (c), and the acausal reflected wave from term $T3$ (d).

als $T1$ and $T2$ are causal, while arrivals $T3$ and $T4$ are acausal. Note that each of the arrivals in Figure 10b corresponds to a stationary source point in Figure 10a. The nonzero portions of these arrivals are due solely to the Fresnel zones around stationary source points. The sources placed at other locations give contributions that interfere destructively.

Figure 11 shows a comparison between the exact waveform for term $T2$, computed with the 2D Green's function (shown with the solid line), and the term $T2$ obtained by summing the correlation over the sources at the surface (shown with crosses). The waveform obtained from seismic interferometry matches the exact waveform well. Note that these waveforms do not look like a Ricker wavelet; as theory predicts, they are shifted with a phase angle equal to $\pi/4$.

Figure 10b shows weak arrivals between $T1$ and $T4$. These weak arrivals arise from endpoint contributions for the sum over the traces of Figure 10a, especially when the arrival time tends to a constant near the endpoints. In the numerical example we tapered the contribution of traces near the endpoints of the source region. Without this tapering these endpoint contributions would be much stronger.

Figure 2 of van Manen et al. (2005) is similar to the correlation gather of Figure 10, except that they used a more complex model of the subsurface that includes a salt dome. Their Figure 3 shows the sum of the correlation gather over the source position, with coherent arrivals in that figure corresponding to the stationary-phase arrivals of their Figure 2. Their example illustrates that the principle of stationary phase can be applied to seismic interferometry in more complex media.

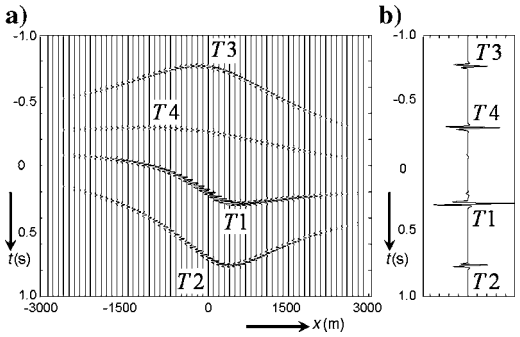

Figure 10. (a) The contribution of sources at the surface to the terms $T1$–$T4$ as a function of the source position x. For clarity only every fifth source position is shown. (b) The sum over all source positions at the surface.

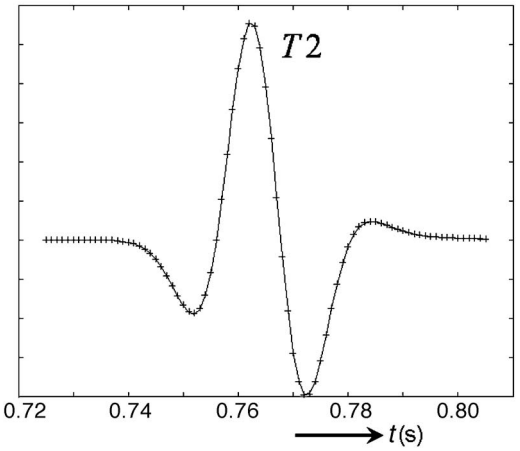

Figure 11. Solid line: exact arrival for term $T2$ computed with the 2D Green's function. The crosses indicate the sum of the correlations for term $T2$ over all sources at the surface. Tapering near the end of the source region was used in the sum.

MODEL WITH MORE THAN ONE REFLECTOR

Up to this point the analysis has been based on the assumption of a single horizontal reflector in the subsurface. Suppose there are more reflectors, at depths D_j with reflection coefficients r_j for downgoing waves. Assuming that the wave velocity remains constant, and considering just the single-reflection contributions to G^{full}, we need to replace the second term in both of equations 10 by a sum over all reflectors. In expression 11, term $T1$ contains the direct waves only. This term is not influenced by the presence of more than one reflector. Terms $T2$ and $T3$ in expression 11 involve the cross-term between the direct wave and the singly reflected waves. Since these terms are linear in the reflection coefficients, one can retrieve the sum of all the singly reflected waves by summing terms $T2$ and $T3$ over the different reflectors. This means that in the presence of more than one reflector, the cross-terms $T2$ and $T3$ between the direct wave and the singly reflected waves produce the full set of single reflections.

Term $T4$ in expression 11 contains the product of the singly reflected waves. This means that for more than one reflector this term contains a double sum $\Sigma_{j,j'} r_j r_{j'}(\ldots)$. This double sum can be split into the terms $j' = j$ and the terms $j \neq j'$:

$$\sum_{j,j'} r_j r_{j'}(\ldots) = \sum_{j} r_j^2(\ldots) + \sum_{j \neq j'} r_j r_{j'}(\ldots). \qquad (39)$$

Strictly speaking, one should include the transmission coefficients t_i of every interface that the waves cross. The transmission coefficients satisfy $t_i = 1 + O(r_i)$. Setting $t_i = 1$ gives a relative error that is of the order r_i. The following treatment therefore is correct up to second order in the reflection coefficients $r_j r_{j'}$.

Analysis of the first term of equation 39 is identical to that of the term $T4$ in the section Analysis of term $T4$. This means that one can sum expression 35 over all reflectors in the subsurface. The last contribution that needs to be accounted for is that of the second sum in the right hand side of equation 39 to the term $T4$. We consider two reflectors, at depths D_1 and D_2 with reflection coefficients r_1 and r_2, respectively. The derivation holds for any pair of reflectors. Representative specular raypaths associated with two different reflectors are shown in Figure 12. The integrand in the term $T4$ of expression 11

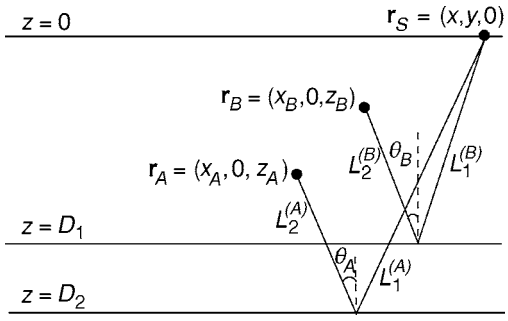

Figure 12. Definition of the geometric variables for the contribution of term $T4$ from waves reflected off two different reflectors.

now contains a phase term exp (ikL) with

$$L = L_1^{(A)} + L_2^{(A)} - L_1^{(B)} - L_2^{(B)}, \tag{40}$$

where these lengths are defined in Figure 12. As before, the phase is stationary with respect to the y-coordinate when $y = 0$. The condition that the phase is stationary with respect to x gives

$$0 = \frac{\partial L}{\partial x} = \sin\,\theta_A - \sin\,\theta_B, \tag{41}$$

where the angles θ_A and θ_B are defined in Figure 12. This follows from the derivation that led to the first term in the right hand side of expression B-10. The stationary-phase condition for this term therefore gives

$$\theta_A = \theta_B, \quad y = 0. \tag{42}$$

Stationary-phase condition 42 gives the two stationary source points $\mathbf{r}_{S1}$ and $\mathbf{r}_{S2}$ at the surface shown in Figure 13. The raypaths shown as solid lines indicate the cross-correlation of the waves that propagate along the following specular trajectories: $\mathbf{r}_{S1}\rightarrow$ reflector 1 $\rightarrow\mathbf{r}_B$ and $\mathbf{r}_{S1}\rightarrow$ reflector $2\rightarrow\mathbf{r}_A$, while the raypaths shown as dashed lines indicate the correlation of the waves that propagate along the following specular trajectories: $\mathbf{r}_{S2}\rightarrow$ reflector 1 $\rightarrow\mathbf{r}_A$ and $\mathbf{r}_{S2}\rightarrow$ reflector $2\rightarrow\mathbf{r}_B$.

The difference in the traveltime of the waves that propagate along the two trajectories shown by the solid lines now differs from the time it takes to propagate between the receivers. The correlation of the waves reflected off different reflectors give stationary-phase contributions that are proportional to the product of reflection coefficients r_1r_2. Hence the correlation of the single-reflected waves from different reflectors gives contributions that dynamically are equivalent to peg-leg multiples that in practice would have been reflected once from a free surface and twice from reflectors in the subsurface, because peg-leg surface multiples are also proportional to r_1r_2.

This may seem a puzzling result, since theory predicts that the full Green's function can be retrieved when the sources are placed on a closed surface that surrounds the region of interest (Wapenaar et al., 2004; Wapenaar et al., 2005). The key point is that in the derivation of this paper the sources are placed at the upper surface only. Let us consider what would happen if we also had sources at a surface $z = z_m$ that is located below the reflectors, as shown in Figure 14.

The reflection and transmission responses of the subsurface are not independent (Claerbout, 1968; Wapenaar et al., 2004). This suggests that sources below the reflectors are again essential for the cancellation of the cross-terms for singly reflected waves; we provide a heuristic argument that this is indeed the case.

Consider the situation in Figure 14 where sources are present at the surface $z = 0$ above the reflectors, and at the surface $z = z_m$ below the reflectors. The points $\mathbf{r}_{S1}$ and $\mathbf{r}_{Sm}$ on these surfaces are the stationary source points for the cross-terms that correspond to the paths indicated with solid lines and dashed lines, respectively. The waves excited at the surface $z = 0$ propagate along the paths shown with solid lines, while the waves excited below the reflectors propagate along the paths shown in dashed lines. These raypaths coincide after their first encounter with reflector 1; hence, the contribution of waves radiated from the stationary points $\mathbf{r}_{S1}$ and $\mathbf{r}_{Sm}$ to the crosscorrelation are nonzero for the same delay time. The contribution of the waves excited at $\mathbf{r}_{S1}$ is proportional to r_1r_2, while the contribution of the waves excited at $\mathbf{r}_{Sm}$ is proportional to $-r_1r_2$ because the reflection coefficient of reflector 1 for a downward reflected waves is $-r_1$

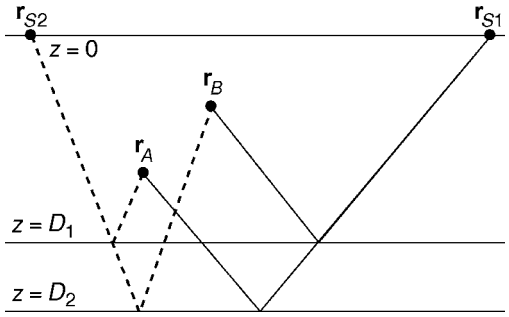

Figure 13. The stationary source points $\mathbf{r}_{S1}$ and $\mathbf{r}_{S2}$ for the correlation of waves reflected from two different reflectors. The corresponding ray paths to the receivers are shown with solid and dashed lines, respectively.

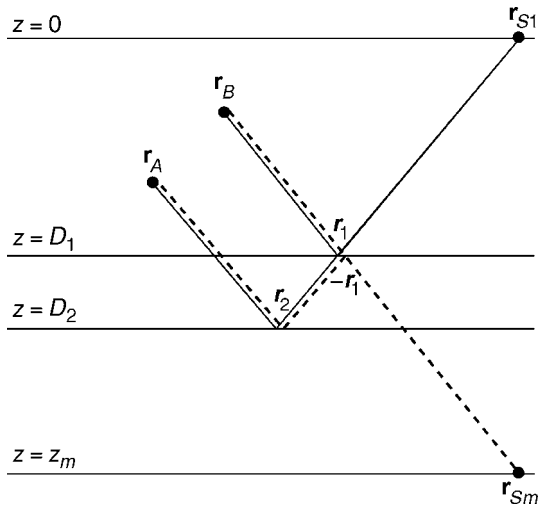

Figure 14. The stationary source points $\mathbf{r}_{S1}$ at the surface $z = 0$ and $\mathbf{r}_{Sm}$ at the surface $z = z_m$ for the correlation of waves reflected from two different reflectors. The corresponding raypaths to the receivers are shown with solid and dashed lines, respectively. The reflection coefficients for the different reflected waves are indicated.

rather than r_1. As shown in the examples in the previous sections, it does not matter how far the stationary point is removed from the surface. Therefore, the stationary points $\mathbf{r}_{S1}$ and $\mathbf{r}_{Sm}$ give contributions to the crosscorrelation that are equal, but have opposite sign. This means that the sum of the cross-terms of the crosscorrelation of these two stationary points gives a vanishing contribution.

In practical situations, the sources may be located at the surface $z = 0$ only. Then the cross-terms of waves reflected from different reflectors give a nonzero contribution that is proportional to the product of reflection coefficients. Therefore, virtual source imaging may introduce events that we call *spurious multiples* when the sources cannot be placed on a closed surface around the region of interest.

CONCLUSION

The main result of this analysis is to demonstrate that the principle of stationary phase underlies seismic interferometry of the direct wave and singly reflected waves. Physically this means that when the contributions from sources on the surface are added, the sources

in the stationary-phase region alone contribute to the emergence of the Green's function.

In the derivation here, we did not explicitly account for the radiation pattern of the point source. It follows from Figure 9 (and Figure A-1 for a heterogeneous medium) that the paths that render the phase of the correlation stationary correspond to rays that propagate in the same direction to the two receivers. This means that if the source does not radiate energy isotropically, the two receivers are still illuminated with the same source strength. Similarly, when the reflection coefficient depends on the angle of incidence, the stationary-phase approximation selects the reflection coefficient at the angle of the reflected wave that propagates between receivers A and B, as shown in Figure 9.

When more reflectors are present, the single-reflection contribution of term $T4$ is proportional to $r_j r_{j'}$. When only sources at the surface $z = 0$ are used, these cross-terms lead to spurious contributions that have the same strength as peg-leg multiples. These spurious multiples are not removed by algorithms for the suppression of surface-related multiples (Verschuur et al., 1992; van Borselen et al., 1996; Dragoset and Jeričević, 1998) because kinematically they do not correspond to peg-leg multiples.

This analysis shows that the Green's function is retrieved from the stationary-phase contribution for the integration (summation) over all sources. Sources far from the stationary point give an oscillatory contribution that averages to zero. When noise, such as swell-noise in the ocean, is used as a source, these sources in general are spread out over the free surface.

The theory presented here sheds light on the conditions that must be satisfied in the practical implementation of seismic interferometry. According to expression 2, the sources must be uncorrelated and must have nearly identical power spectra. Man-made sources that are fired sequentially are certainly uncorrelated. Care must be taken that these also have nearly identical power spectra. Natural sources, such as noise generated by turbulent waves at the ocean surface, have a finite correlation length. The theory presented here is valid only when this correlation length is much smaller than the wavelength of the sound waves that are generated. We assumed in the analysis that the source density n is constant. This is true only when the sources are stationary in space. These complications need to be addressed in practical implementations of seismic interferometry.

ACKNOWLEDGMENTS

We appreciate the enlightening comments of Rodney Calvert, Andrew Curtis, Kurang Mehta, Johan Robertsson, John Stockwell, and an anonymous reviewer. This work was supported by the Consortium Project on Seismic Inverse Methods for Complex Structures at CWP and by the Netherlands Research Centre for Integrated Solid Earth Science (ISES).

APPENDIX A

SEISMIC INTERFEROMETRY OF THE DIRECT WAVES IN THE RAY-GEOMETRIC APPROXIMATION

In this appendix, we show that the arguments used in this paper for a homogeneous medium can be generalized to heterogenous media where the velocity and density variations are sufficiently smooth to justify the use of ray theory for the Green's function. To avoid complications due to curved reflectors, we analyze only term $T1$. The ray-geometric Green's function that gives the response at $\mathbf{r}_1$ due to a point source at $\mathbf{r}_2$ is given by expression 15 of Snieder and Chapman (1998):

$$G^{\text{ray}}(\mathbf{r}_1,\mathbf{r}_2) = -\frac{1}{4\pi}\sqrt{\frac{\rho_1\rho_2 v_1}{v_2}}\frac{\exp(i\omega\tau_{12})}{\sqrt{J_{12}}}. \qquad \text{(A-1)}$$

In expression A-1, $v_1 = v(\mathbf{r}_1)$, and we use a similar notation for the density, τ_{12} is the traveltime for the propagation from $\mathbf{r}_2$ to $\mathbf{r}_1$, and J_{12} is the associated geometrical-spreading factor. Because of reciprocity (Snieder and Chapman, 1998), this Green's function is also equal to

$$G^{\text{ray}}(\mathbf{r}_1,\mathbf{r}_2) = -\frac{1}{4\pi}\sqrt{\frac{\rho_1\rho_2 v_2}{v_1}}\frac{\exp(i\omega\tau_{21})}{\sqrt{J_{21}}}. \qquad \text{(A-2)}$$

Note that the traveltime is reciprocal:

$$\tau_{12} = \tau_{21}, \qquad \text{(A-3)}$$

but the geometrical spreading is not (Snieder and Chapman, 1998).

Inserting Green's function A-2 in term $T1$ of expression 11 gives

$$T1 = \frac{1}{(4\pi)^2}\int\frac{\sqrt{\rho_A\rho_B}\rho_S v_S}{\sqrt{v_A v_B}}\frac{\exp(i\omega(\tau_{SA}-\tau_{SB}))}{\sqrt{J_{SA}J_{SB}}}dxdy, \qquad \text{(A-4)}$$

where $v_S = v(\mathbf{r}_S) = v(x,y,0)$, $v_A = v(\mathbf{r}_A)$, and $v_B = v(\mathbf{r}_B)$. By analogy with the situation shown in Figure 3, the stationary points in this integral correspond to the rays that propagate from the source S through receiver B to receiver A, as shown in Figure A-1. By virtue of reciprocity, these stationary points can be found by tracing rays from receiver A to receiver B and continuing these rays to the surface $z = 0$. In general there may be more than one stationary point. In the following, we analyze the contribution of just one stationary point, but ultimately one needs to sum over all stationary points. It may happen, in fact, that the region of stationary phase does not consist of a finite number of points, but of a line or surface area. Then, point A is a caustic and ray theory breaks down (Berry and Upstill, 1980).

Let the traveltime along the ray from A to B to S be given by τ_0. The traveltime for an adjacent ray follows from the second-order Taylor expansion in the ray-centered coordinates q_1 and q_2 that measure the perpendicular distance to the ray in two orthogonal directions. According to expression 50 of Červený and Hron (1980), the traveltime along an adjacent ray is given by

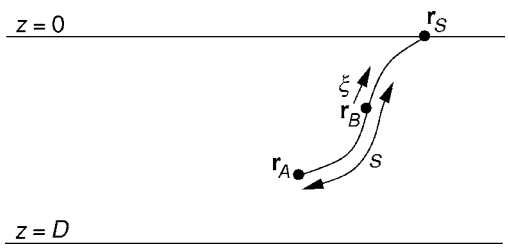

Figure A-1. The stationary-phase condition for term $T1$ for a heterogeneous reference medium.

$$\tau = \tau_0 + \frac{1}{2}\mathbf{q}\cdot\mathbf{M}\cdot\mathbf{q}, \tag{A-5}$$

with $\mathbf{M}$ a matrix of second-order derivatives of the traveltime. In the following, it is convenient to replace the integration over the surface $z = 0$ in expression A-4 by an integration over the ray-centered coordinates q_1 and q_2. The orientation of these coordinate axes is ambiguous, since any choice of axes perpendicular to the ray is admissible. In the following we choose the q_2-axis to be aligned with the plane $z = 0$, as indicated in Figure A-2. The other coordinate, q_1, then measures the distance to the ray in the orthogonal direction. As shown in Figure A-2, the associated q_1-axis makes an angle ψ with the horizontal that is equal to the angle between the ray and the vertical. An element dq_2 corresponds to an element dy' in the x,y-plane, while an element dq_1 corresponds to an element $dq_1 = \cos\psi dx'$. We use primed coordinates since the ray direction is not necessarily aligned with the original x-axis. This means that a surface element in the surface integral can be related to a surface element dq_1dq_2 using

$$dxdy = dx'dy' = \frac{1}{\cos\psi}dq_1dq_2. \tag{A-6}$$

This expression can be used to evaluate integral A-4 in the stationary-phase approximation. With Taylor expansion A-5 for the rays from A to S and from B to S, this integral in the stationary-phase approximation is given by

$$T1 = \frac{1}{(4\pi)^2\cos\psi}\frac{\sqrt{\rho_A\rho_B}\rho_S v_S}{\sqrt{v_A v_B}}\frac{\exp(i\omega(\tau_{SA}-\tau_{SB}))}{\sqrt{J_{SA}J_{SB}}} \times\int\exp\left(\frac{i\omega}{2}\mathbf{q}\cdot(\mathbf{M}_{SA}-\mathbf{M}_{SB})\cdot\mathbf{q}\right)dq_1dq_2. \tag{A-7}$$

The integration over the q-variables gives (Bleistein, 1984)

$$T1 = \frac{1}{8\pi\omega\cos\psi}\frac{\sqrt{\rho_A\rho_B}\rho_S v_S}{\sqrt{v_A v_B}}\frac{\exp(i\omega(\tau_{SA}-\tau_{SB}))}{\sqrt{J_{SA}J_{SB}}} \times\frac{\exp(isgn\pi/4)}{\sqrt{|\det(\mathbf{M}_{SA}-\mathbf{M}_{SB})|}}, \tag{A-8}$$

where sgn is the number of positive eigenvalues of $\mathbf{M}_{SA}-\mathbf{M}_{SB}$ minus the number of negative eigenvalues. Using the same reasoning as in the derivation of expression 6.21 of Snieder and Lomax (1996), term $T1$ is equal to

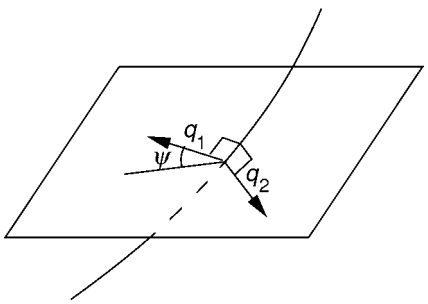

Figure A-2. Definition of the ray-centered coordinates q_1 and q_2. The q_2-axis lies in the x,y-plane and is perpendicular to the ray. The angle ψ is the angle between the ray direction and the vertical.

$$T1 = \frac{i}{8\pi\omega\cos\psi}\frac{\sqrt{\rho_A\rho_B}\rho_S v_S}{\sqrt{v_A v_B}}\frac{\exp(i\omega(\tau_{SA}-\tau_{SB}))}{\sqrt{J_{SA}J_{SB}\det(\mathbf{M}_{SA}-\mathbf{M}_{SB})}}. \tag{A-9}$$

Since the points $\mathbf{r}_A$, $\mathbf{r}_B$, and $\mathbf{r}_S$ are located on the same ray,

$$\tau_{SA}-\tau_{SB} = \tau_{AB}, \tag{A-10}$$

this is the traveltime along the ray that joins receivers A and B. This means that term $T1$ is kinematically identical to the Green's function that accounts for wave propagation between the receivers A and B. In the following, we show that expression A-9 also accounts dynamically for this Green's function by using a derivation similar to that presented by Snieder and Lomax (1996).

According to expression 68 of Cervený and Hron (1980), matrix $\mathbf{M}$ is related to the curvature matrix of the wavefronts by the relation

$$\mathbf{M} = \frac{1}{v}\mathbf{K}. \tag{A-11}$$

Because $\mathbf{M}$ is a 2×2 matrix, this, together with expression A-10, implies that

$$T1 = \frac{i}{8\pi\omega\cos\psi}\frac{\sqrt{\rho_A\rho_B}\rho_S v_S^2}{\sqrt{v_A v_B}}\frac{\exp(i\omega\tau_{AB})}{\sqrt{J_{SA}J_{SB}\det(\mathbf{K}_{SA}-\mathbf{K}_{SB})}}. \tag{A-12}$$

Following equation 76 of Cervený and Hron (1980), the curvature matrix satisfies the following matrix Ricatti equation:

$$\frac{d\mathbf{K}_{SA}}{ds} = \frac{1}{v}\frac{dv}{ds}\mathbf{K}_{SA} - \mathbf{K}_{SA}^2 - \frac{1}{v}\mathbf{V}, \tag{A-13}$$

where $v = v_S$, and the matrix $\mathbf{V}$ is defined by $V_{ij} = \partial^2 v/\partial q_i\partial q_j$, and where s is the distance along the ray from $\mathbf{r}_A$ through $\mathbf{r}_B$ to the surface, as indicated in Figure A-1. Using this expression, and the corresponding expression for $\mathbf{K}_{SB}$, it follows that the difference satisfies the differential equation

$$\frac{d(\mathbf{K}_{SA}-\mathbf{K}_{SB})}{ds} = \frac{1}{v}\frac{dv}{ds}(\mathbf{K}_{SA}-\mathbf{K}_{SB}) - (\mathbf{K}_{SA}^2-\mathbf{K}_{SB}^2). \tag{A-14}$$

From this it follows after a lengthy calculation that

$$\frac{d}{ds}\det(\mathbf{K}_{SA}-\mathbf{K}_{SB}) = \frac{2}{v}\frac{dv}{ds}\det(\mathbf{K}_{SA}-\mathbf{K}_{SB}) - (tr\,\mathbf{K}_{SA} + tr\,\mathbf{K}_{SB})\det(\mathbf{K}_{SA}-\mathbf{K}_{SB}), \tag{A-15}$$

where tr denotes the trace. According to expression 36 of Snieder and Chapman (1998)

$$tr\,\mathbf{K} = \frac{1}{J}\frac{dJ}{ds}. \tag{A-16}$$

Using this expression to eliminate the trace of $\mathbf{K}_{SA}$ and $\mathbf{K}_{SB}$ from expression A-15, we can integrate the result to give

$$\frac{d}{ds}\left\{\frac{J_{SA}J_{SB}\det(\mathbf{K}_{SA}-\mathbf{K}_{SB})}{v_S^2}\right\}=0 \qquad \text{(A-17)}$$

or

$$\frac{J_{SA}J_{SB}\det(\mathbf{K}_{SA}-\mathbf{K}_{SB})}{v_S^2}=\text{const.} \qquad \text{(A-18)}$$

This expression holds for any point S along the ray in Figure A-1. The constant can be found by evaluating this expression for a point S along the ray at a small distance ξ beyond the receiver B, as shown in Figure A-1, and by letting this distance go to zero. At a small distance from receiver B, the medium can be considered to be locally homogeneous, and the curvature matrix attains its value for a homogeneous medium:

$$\mathbf{K}_{SB}=\begin{vmatrix}1/\xi & 0\\ 0 & 1/\xi\end{vmatrix}. \qquad \text{(A-19)}$$

In the limit $\xi\rightarrow 0$ these terms dominate the contributions from $\mathbf{K}_{SA}$ in expression A-18 and $\det(\mathbf{K}_{SA}-\mathbf{K}_{SB})\rightarrow 1/\xi^2$ as $\xi\rightarrow 0$. In that limit, the geometrical spreading is given by $J_{SB}=\xi^2, J_{SA}\rightarrow J_{BA}$, and $v_S\rightarrow v_B$. Inserting these results in expression A-12 shows that the constant in that expression is given by const $= J_{BA}/v_B^2$. Inserting this in expression A-18 finally gives

$$J_{SA}J_{SB}\det(\mathbf{K}_{SA}-\mathbf{K}_{SB})=\frac{v_S^2}{v_B^2}J_{BA} \qquad \text{(A-20)}$$

or

$$\sqrt{J_{SA}J_{SB}\det(\mathbf{K}_{SA}-\mathbf{K}_{SB})}=\pm\frac{v_S}{v_B}\sqrt{J_{BA}}. \qquad \text{(A-21)}$$

At this point, the sign in the right hand side is arbitrary.

This last result can be used to eliminate $\sqrt{\det(\mathbf{K}_{SA}-\mathbf{K}_{SB})}$ from expression A-12, giving

$$T1=\frac{\pm i\rho_S v_S}{8\pi\omega\cos\psi}\sqrt{\frac{\rho_A\rho_B v_B}{v_A}}\frac{\exp(i\omega\tau_{AB})}{\sqrt{J_{BA}}}. \qquad \text{(A-22)}$$

Following expression 45 of Snieder and Chapman (1998), the reciprocity property of the geometrical spreading is given by $J_{BA}=(v_B/v_A)^2J_{AB}$; hence,

$$T1=\frac{\pm i\rho_S v_S}{8\pi\omega\cos\psi}\sqrt{\frac{\rho_A\rho_B v_A}{v_B}}\frac{\exp(i\omega\tau_{AB})}{\sqrt{J_{AB}}}. \qquad \text{(A-23)}$$

Comparison with the ray-geometric Green's function A-1 gives

$$T1=\frac{\mp\rho_S v_S}{2\cos\psi}\times\frac{G^{ray}(\mathbf{r}_A,\mathbf{r}_B)}{-i\omega}. \qquad \text{(A-24)}$$

After multiplying with the terms $n|S(\omega)|^2$, this result can directly be compared with the corresponding expression 21 for a homogeneous medium. This implies that the lower sign in expression A-21 must be used. After taking the source spectrum and the scatterer density into account, this finally gives equation 23.

APPENDIX B

COMPUTATION OF THE PATH LENGTH AND ITS DERIVATIVES

Before we can analyze expression 24 we need the coordinates of the reflection point $\mathbf{r}_R$ because this determines the lengths L_1 and L_2. Using the geometric variables defined in Figure B-1, the condition that the reflection angle is equal to the angle of incidence gives

$$x_R=\frac{(D-z_A)x+Dx_A}{2D-z_A},$$
$$y_R=\frac{(D-z_A)y}{2D-z_A}. \qquad \text{(B-1)}$$

Using this, the lengths $L_1$and L_2 are given by

$$L_1=\sqrt{\left(\frac{D}{2D-z_A}\right)^2(x-x_A)^2+\left(\frac{D}{2D-z_A}\right)^2y^2+D^2} \qquad \text{(B-2)}$$

and

$$L_2=\sqrt{\left(\frac{D-z_A}{2D-z_A}\right)^2(x-x_A)^2+\left(\frac{D-z_A}{2D-z_A}\right)^2y^2+(D-z_A)^2}, \qquad \text{(B-3)}$$

while L_B is given by expression 13.

The stationary points of integral 24 follow from the first partial derivatives of $L=L_1+L_2-L_B$:

$$0=\frac{\partial L}{\partial y}=\left(\frac{D}{2D-z_A}\right)^2\left(\frac{y}{L_1}\right)+\left(\frac{D-z_A}{2D-z_A}\right)^2\left(\frac{y}{L_2}\right)-\frac{y}{L_B}. \qquad \text{(B-4)}$$

Again, the stationary-source position occurs for $y=0$; it is located in the vertical plane of the receivers. The condition for stationarity in the x-direction is

$$0=\frac{\partial L}{\partial x}=\left(\frac{D}{2D-z_A}\right)^2\left(\frac{x-x_A}{L_1}\right)+\left(\frac{D-z_A}{2D-z_A}\right)^2\left(\frac{x-x_A}{L_2}\right)-\frac{x-x_B}{L_B}. \qquad \text{(B-5)}$$

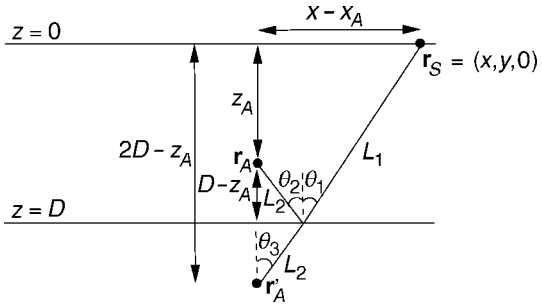

Figure B-1. The angles θ_1, θ_2, and θ_3, and their relation to the geometric variables for the reflected wave.

In order to interpret this last condition geometrically, it is useful to relate the ratios in this expression to the angle of incidence at the reflector. Referring to Figure B-1, the following identities hold: $\cos\theta_1 = D/L_1$, $\cos\theta_2 = (D - z_A)/L_2$, and $\cos\theta_3 = (2D - z_A)/(L_1 + L_2)$. Since these angles are all equal to the angle of incidence θ_A of the reflected wave, we obtain:

$$\cos\theta_A = \frac{D}{L_1} = \frac{D - z_A}{L_2} = \frac{2D - z_A}{L_1 + L_2}. \quad \text{(B-6)}$$

Also, since $x - x_A = L_1 \sin\theta_1 + L_2 \sin\theta_2$, and since both angles are equal to θ_A,

$$\sin\theta_A = \frac{x - x_A}{L_1 + L_2}. \quad \text{(B-7)}$$

Dividing this expression by the last identity of equation B-6 gives

$$\tan\theta_A = \frac{x - x_A}{2D - z_A}. \quad \text{(B-8)}$$

Finally, from expression B-6,

$$\frac{D}{2D - z_A} = \frac{L_1}{L_1 + L_2}, \quad \frac{D - z_A}{2D - z_A} = \frac{L_2}{L_1 + L_2}. \quad \text{(B-9)}$$

Using expression B-9 in expression B-5, and using equation B-7 to eliminate $x - x_A$, gives, with the relation $(x - x_B)/L_B = \sin\psi_B$,

$$0 = \frac{\partial L}{\partial x} = \sin\theta_A - \sin\psi_B. \quad \text{(B-10)}$$

The integrand thus is stationary when the source position satisfies equation 25.

From expression B-2 we get at, the stationary point,

$$\frac{\partial^2 L_1}{\partial x^2} = \left(\frac{D}{2D - z_A}\right)^2 \frac{D^2}{L_1^3} = \left(\frac{L_1}{L_1 + L_2}\right)^2 \frac{D^2}{L_1^2}\frac{1}{L_1} = \frac{L_1}{(L_1 + L_2)^2}\cos^2\theta. \quad \text{(B-11)}$$

In the second identity we have used expression B-9, while the last identity follows from equation B-6. In a similar way it follows that

$$\frac{\partial^2 L_2}{\partial x^2} = \frac{L_2}{(L_1 + L_2)^2}\cos^2\theta, \quad \text{(B-12)}$$

and, using equation 17, we obtain for the curvature of L_B,

$$\frac{\partial^2 L_B}{\partial x^2} = \frac{1}{L_B}\cos^2\theta. \quad \text{(B-13)}$$

In this last expression, we used the stationary-phase condition $\psi = \theta$. Combining these results in the path difference $L = L_1 + L_2 - L_B$ gives equation 26.

Differentiation of equation B-2 gives

$$\frac{\partial^2 L_1}{\partial y^2} = \left\{\left(\frac{D}{2D - z_A}\right)^4 (x - x_A)^2 + \left(\frac{D}{2D - z_A}\right)^2 D^2\right\}/L_1^3. \quad \text{(B-14)}$$

With expressions B-8 and B-9, this is equal to

$$\frac{\partial^2 L_1}{\partial y^2} = \left(\frac{D}{L_1}\right)^2 \frac{1}{L_1}\left(\frac{L_1}{L_1 + L_2}\right)^2 (\tan^2\theta + 1). \quad \text{(B-15)}$$

Using the identity $D/L_1 = \cos\theta$, this gives

$$\frac{\partial^2 L_1}{\partial y^2} = \frac{L_1}{(L_1 + L_2)^2}. \quad \text{(B-16)}$$

A similar analysis for L_2 gives

$$\frac{\partial^2 L_2}{\partial y^2} = \frac{L_2}{(L_1 + L_2)^2}. \quad \text{(B-17)}$$

This gives expression 27, for the curvature of L in the y-direction.

REFERENCES

Bakulin, A., and R. Calvert, 2004, Virtual source: New method for imaging and 4D below complex overburden: 74th Annual International Meeting, SEG, Expanded Abstracts, 2477–2480.

Berry, M., and C. Upstill, 1980, Catastrophe optics: Morphologies of caustics and their diffraction patterns, *in* E. Wolf, ed., Progress in optics, XVIII, 257–346.

Bleistein, N., 1984, Mathematical methods for wave phenomena: Academic Press Inc.

Bleistein, N., J. K. Cohen, and J. W. Stockwell Jr., 2001, Mathematics of multidimensional seismic imaging, migration, and inversion: Springer Publishing Company, Inc.

Calvert, R. W., A. Bakulin, and T. C. Jones, 2004, Virtual sources, a new way to remove overburden problems, 66th Annual International Meeting, EAEG, Expanded Abstracts, 234.

Campillo, M., and A. Paul, 2003, Long-range correlations in the diffuse seismic coda: Science, **299**, 547–549.

Cervený, V., and F. Hron, 1980, The ray series method and dynamical ray tracing system for three-dimensional inhomogeneous media: Bulletin of the Seismological Society of America, **70**, 47–77.

Claerbout, J. F., 1968, Synthesis of a layered medium from its acoustic transmission response: Geophysics, **33**, 264–269.

Derode, A., E. Larose, M. Campillo, and M. Fink, 2003a, How to estimate the Green's function for a heterogeneous medium between two passive sensors? Application to acoustic waves: Applied Physics Letters, **83**, 3054–3056.

Derode, A., E. Larose, M. Tanter, J. de Rosny, A. Tourin, M. Campillo, and M. Fink, 2003b, Recovering the Green's function from far-field correlations in an open scattering medium: Journal of the Acoustic Society of America, **113**, 2973–2976.

Dragoset, W. H., and Z. Jeričević, 1998, Some remarks on multiple attenuation: Geophysics, **63**, 772–789.

Haney, M., R. Snieder, and J. Sheiman, 2005, Further thoughts on the stacking response in seismic data processing: First Break, **23**, 35–38.

Larose, E., A. Derode, M. Campillo, and M. Fink, 2004, Imaging from one-bit correlations of wideband diffuse wave fields: Journal of Applied Physics, **95**, 8393–8399.

Lobkis, O. I., and R. L. Weaver, 2001, On the emergence of the Green's function in the correlations of a diffuse field: Journal of the Acoustic Society of America, **110**, 3011–3017.

Malcolm, A., J. Scales, and B. A. van Tiggelen, 2004, Extracting the Green's function from diffuse, equipartitioned waves: Physical Review E, **70**, 015601.

Rickett, J. E., and J. F. Claerbout, 1999, Acoustic daylight imaging via spectral factorization; Helioseismology and reservoir monitoring: The Leading Edge, **18**, 957–960.

———, 2000, Calculation of the sun's acoustic impulse response by multidimensional spectral factorization: Solar Physics, **192**, 203–210.

Roux, P., and M. Fink, 2003, Green's function estimation using secondary sources in a shallow water environment: Journal of the Acoustic Society of America, **113**, 1406–1416.

Roux, P., K. G. Sabra, W. A. Kuperman, and A. Roux, 2005, Ambient noise

cross correlation in free space: Theoretical approach: Journal of the Acoustic Society of America, **117**, 79–84.
Sabra, K. G., P. Roux, and W. A. Kuperman, 2005, Arrival-time structure of the time-averaged ambient noise cross-correlation in an oceanic waveguide: Journal of the Acoustic Society of America, **117**, 164–174.
Schuster, G. T., 2001, Theory of daylight/interferometric imaging: Tutorial: 63rd Annual International Meeting, EAGE, Extended Abstracts, Session A32.
Schuster, G. T., J. Yu, J. Sheng, and J. Rickett, 2004, Interferometric/daylight seismic imaging: Geophysical Journal International, **157**, 838–852.
Shapiro, N. M., and M. Campillo, 2004, Emergence of broadband Rayleigh waves from correlations of the ambient seismic noise: Geophysical Research Letters, **31**, L07614, .
Shapiro, N. M., M. Campillo, L. Stehly, and M. H. Ritzwoller, 2005, High-resolution surface-wave tomography from ambient seismic noise: Science, **307**, 1615–1618.
Snieder, R., 2004a, Extracting the Green's function from the correlation of coda waves: A derivation based on stationary phase: Physical Review E, **69**, 046610.
———, 2004b, A guided tour of mathematical methods for the physical sciences: 2nd ed.: Cambridge University Press.
Snieder, R., and C. Chapman, 1998, The reciprocity properties of geometrical spreading: Geophysical Journal International, **132**, 89–95.
Snieder, R., and A. Lomax, 1996, Wavefield smoothing and the effect of rough velocity perturbations on arrival times and amplitudes: Geophysical Journal International, **125**, 796–812.
Snieder, R., and E. Şafak, 2006, Extracting the building response from an incoherent excitation; Theory and application to the Millikan Library in Pasadena, California: Bulletin of the Seismological Society of America, **96**, 586–598.
Snieder, R., J. Sheiman, and R. Calvert, 2006, Equivalence of the virtual source method and wavefield deconvolution in seismic interferometry: Physical Review E, **73**, 066620.
van Borselen, R. G., J. T. Fokkema, and P. M. van den Berg, 1996, Removal of surface-related wave phenomena — The marine case: Geophysics, **61**, 202–210.
van Manen, D. J., J. O. A. Robertsson, and A. Curtis, 2005, Modelling of wave propagation in inhomogeneous media: Physical Review Letters, **94**, 164301.
Verschuur, D. J., A. J. Berkhout, and C. P. A. Wapenaar, 1992, Adaptive surface-related multiple elimination: Geophysics, **57**, 1166–1177.
Wapenaar, K., 2004, Retrieving the elastodynamic Green's function of an arbitrary inhomogeneous medium by cross correlation: Physical Review Letters, **93**, 254301.
Wapenaar, K., D. Draganov, J. Thorbecke, and J. Fokkema, 2002, Theory of acoustic daylight imaging revisited: 72nd Annual International Meeting, SEG, Expanded Abstracts, 2269–2272.
Wapenaar, K., J. Fokkema, and R. Snieder, 2005, Retrieving the Green's function by cross-correlation: A comparison of approaches: Journal of the Acoustic Society of America, **118**, 2783–2786.
Wapenaar, K., J. Thorbecke, and D. Dragonov, 2004, Relations between reflection and transmission responses of 3D inhomogeneous media: Geophysical Journal International, **156**, 179–194.
Weaver, R. L., and O. I. Lobkis, 2001, Ultrasonics without a source: Thermal fluctuation correlations and MHz frequencies: Physical Review Letters, **87**, 134301–1/4.
———, 2004, Diffuse fields in open systems and the emergence of the Green's function: Journal of the Acoustic Society of America, **116**, 2731–2734.
Yilmaz, O., 1987, Seismic data processing: SEG Investigations in geophysics 2.